

Neutron Diffraction and Finite-Element Analysis of Thermal Residual Stresses on Diffusion-Bonded Silicon Carbide-Molybdenum Joints

Antonio E. Martinelli[†] and Robin A. L. Drew^{*:‡}

Department of Mining and Metallurgical Engineering, McGill University, Montreal, QC, H3A 2B2, Canada

Eduardo A. Fancello

Department of Mechanical Engineering, Universidade Federal de Santa Catarina, Florianópolis, SC, 88040-900, Brazil

Ronald Rogge and John H. Root

Atomic Energy of Canada, Ltd., Neutron and Condensed Matter Science Branch, Chalk River Laboratories, Chalk River, ON, K0J 1J0 Canada

Various approaches can be used to minimize residual stresses in ceramic-metal joining, such as a refractory-metal interlayer in a hot-pressed joint. Nonetheless, it is still necessary to characterize the stresses at and near the interface between the interlayer and the ceramic, as a function of the hot-pressing parameters. This study combines two techniques to assess the stress distribution of hot-pressed silicon carbide-molybdenum joints: neutron diffraction and finite-element (FEM) analysis. The results demonstrate that the joining temperature greatly influences the final stress distribution, and that significant stress accommodation is achieved by controlling the cooling rate of the diffusion couples. FEM analysis provides a broad view of stress distribution profiles, whereas experimental stress values that are obtained via neutron diffraction allow a better assessment of the effects of parameters that are not easily reproduced using a mathematical model.

I. Introduction

CERAMICS such as SiC and Si₃N₄ are characterized by high strength at high temperatures, good wear resistance, and excellent chemical stability, in comparison to conventional metals and structural alloys. They are suitable materials for high-temperature applications and chemically hostile environments. However, because of their brittle behavior, the use of ceramics usually is restricted to specific components that commonly are attached to metallic parts. Among the various methods that are currently available to produce sound ceramic-metal joints, solid-state diffusion bonding is known to produce interfaces that are capable of resisting high temperatures and chemical attack, exceeding the capabilities of brazed joints.^{1,2} Nevertheless, a critical problem concerning solid-state diffu-

sion is related to the different thermal expansion behaviors of the materials. Highly covalent ceramics, such as SiC and Si₃N₄, invariably have lower coefficients of thermal expansion (CTE) than metals. Si₃N₄ and SiC have CTEs of $3.5 \times 10^{-6}/^{\circ}\text{C}$ and $4.4 \times 10^{-6}/^{\circ}\text{C}$ respectively, whereas metals and alloys have CTEs ranging from $8 \times 10^{-6}/^{\circ}\text{C}$ up to $25 \times 10^{-6}/^{\circ}\text{C}$.³ Consequently, residual stresses are generated during cooling of the diffusion couple from relatively high bonding temperatures, thus affecting the mechanical integrity of the joint. Several approaches can be used to overcome this problem, such as the use of metallic interlayers between the ceramic and the base metal. From the standpoint of thermal expansion, refractory metals such as tungsten (CTE = $4.5 \times 10^{-6}/^{\circ}\text{C}$) and molybdenum (CTE = $5.4 \times 10^{-6}/^{\circ}\text{C}$) are the most attractive materials for use as interlayers for joining SiC and Si₃N₄ to other metals. Their CTEs are similar to those of ceramics and they can be used to reduce the thermal mismatch between SiC/Si₃N₄ and metals or metal alloys with higher CTE values. However, it is necessary to assess the potential of a specific interlayer. In addition to microstructural characterization and mechanical strength, the formation of residual stresses between the interlayer and the ceramic (and ways to minimize their amplitude) is a major task.

The interface microstructure⁴⁻⁸ and joint strength⁹ of SiC-Mo joining couples have been studied in some detail. However, no study has been conducted on the determination of residual stresses. Stress distributions of hot-pressed diffusion couples have been obtained for other ceramic-metal systems such as Si₃N₄-stainless steel, using only finite-element (FEM) analysis.¹⁰ Despite the fact that numerical models usually provide reliable approximations, important aspects such as the cooling rate are not considered. In FEM analysis, mathematical data are readily gathered, allowing an overall view of stress distribution profiles; however, construction of the model requires several assumptions that concern material properties and a simplification of the mechanisms that are involved in the joining process. On the other hand, experimental stress values allow an assessment of the effects of parameters that are not easily studied via a mathematical analysis, resulting in an actual description of the joining process. However, the values are generally characterized by large errors that are characteristic of the measurement process and sample size; hence, data collection may become time consuming and rather expensive. Therefore, the objective of this work was to evaluate the distribution of thermomechanical stresses in pressureless-sintered SiC diffusion-bonded to molybdenum, using both the numerical analysis (FEM) and an experimental approach (neutron diffraction), and to provide a comparison of the two methods.

J. J. Petrovic—contributing editor

Manuscript No. 190605. Received October 27, 1997; approved December 3, 1998.

Supported by NSERC-Canada and CNPq-Brazil.

[†]Member, American Ceramic Society.

[‡]Currently with Dept. of Physics, Universidade Federal do Rio Grande do Norte, Lagoa Nova Campus, Nata, RN, 59072-970, Brazil.

^{*}Author to whom correspondence should be addressed (E-mail address: Robin@MinMet.Lan.McGill.Ca).

II. Joining of SiC-Mo Diffusion Couples

SiC-Mo diffusion couples were prepared, using pressureless-sintered hexagonal α -SiC (Hexoloy-grade SATM, Carborundum Co., Niagara Falls, NY) and molybdenum sheet metal (99.95% pure, Johnson & Matthey, Toronto, Canada). The samples consisted of a block of SiC that was mounted on a block of molybdenum that had a cross-sectional area of 9.0 mm \times 9.0 mm and thicknesses of 6 and 2.5 mm, for SiC and molybdenum, respectively. The surfaces to be joined were ground and polished to a 1.0 μ m finish with diamond paste and cleaned ultrasonically in isopropanol for 5 min. Individual samples were inserted in a graphite die, embedded in BN powder (99.5% pure, Johnson & Matthey), and placed in a hot press. Calibration of the load cell was performed periodically; a precision of 5% of the nominal applied load was maintained. The sample temperature was measured by using an infrared pyrometer (Model M-600, Mikron Instrument Co., Oakland, NJ) that was inserted in the back of the furnace and calibrated against a type-C thermocouple that was placed in contact with the sample. Hence, the test temperatures were $\pm 5^\circ\text{C}$ of the nominal value.

SiC-Mo diffusion couples were hot-pressed in a vacuum of 2×10^{-4} atm (20 Pa) or better. The joining temperatures varied over a range of 1200–1400°C, and the soaking time was set to 1 h. During that period, a uniaxial pressure of 10 MPa was applied to the samples. After the vacuum was established in the furnace chamber, the sample was heated to the preset joining temperature at a rate of 15°C/min. When the sample temperature was 10°C lower than the set point, the load was applied to the sample. After 1 h, the sample was cooled to room temperature. The applied load was carefully removed during the initial stages of cooling. Two cooling profiles were used; they are labeled “A” and “B” in Fig. 1. In profile A, the sample was simply furnace cooled, resulting in relatively high initial cooling rates, because the hot-pressing chamber was water cooled. Profile B consisted of cooling the sample slowly (5°C/min) for the first 500°C; then, the sample was furnace cooled for the remainder of the cycle.

III. Neutron-Diffraction Analysis

Thermal residual stresses in SiC-Mo joints were studied via neutron diffraction at the AECL (Atomic Energy of Canada, Ltd.) facilities in Chalk River, Canada. Neutrons generated in the nuclear reactor were collimated toward a germanium crystal, which generated a monochromatic beam (wavelength, λ , of 1.8533 Å). The neutron beam was then collimated again toward a SiC-Mo sample that was placed on top of a moving table. The spacial position of the sample was adjusted by a set of independent stages for the x -, y -, and z -coordinates. The x - and

y -coordinates were variable (the analysis coordinates) and the z -coordinate was fixed. The beam height was greater than the sample height, which allowed an integrated diffraction process through the entire sample, i.e., along the y -axis. The stresses on the SiC side of the samples were studied using the (212) planes, which diffracted at an angle $\phi = -89.84^\circ$, where

$$\phi = 2\theta \quad (1)$$

θ is the Bragg angle.

For molybdenum, the (211) planes were used, corresponding to $\phi = -92.40^\circ$. These particular sets of planes were chosen, considering the intensity of the diffracted peak (relatively high) and its angular position ($\phi \approx 90^\circ$), to minimize the distortion of the sampling volume, which was $\sim 5 \text{ mm} \times 5 \text{ mm}$ and had the same thickness as that of the sample.

Strains were defined as¹¹

$$\epsilon = \frac{d - d_0}{d_0} \quad (2)$$

where d corresponds to the spacing between a particular set of crystallographic planes under tension or compression. When the material is under tension, the planes are pulled slightly apart so that d increases with respect to a strain-free value, d_0 . Similarly, if the sample is under compression, the planes are pushed together and d decreases with respect to d_0 . The angle of rotation (Ψ) of the table was adjusted to select the geometry of the diffraction process and, therefore, the component of strain to be studied. The normal component of strain (ϵ_z) was studied by setting the Ψ value of the sample equal to $\phi/2$, and the in-plane component (ϵ_x) was studied by setting Ψ equal to $\phi/2 + 90^\circ$. Therefore, the corresponding values of Ψ for SiC were 45.08° for the in-plane component and -44.92° for the normal component. For molybdenum, Ψ was equal to 43.80° for the in-plane component and -46.20° for the normal component.

After the strains were obtained, the stresses were calculated, according to

$$\sigma_x = \frac{E}{1 + \nu} \left[\epsilon_x + \frac{\nu}{1 - 2\nu} (\epsilon_x + \epsilon_y + \epsilon_z) \right] \quad (3)$$

where E is the elastic modulus and ν is the Poisson's ratio. The room-temperature E values for SiC and molybdenum are 414 and 324 GPa, respectively. As for ν , the values used were 0.14 for SiC¹² and 0.324 for molybdenum.¹³ A cyclic permutation of indices in Eq. (3) yielded the other two components of stress (σ_y and σ_z). On the basis of sample symmetry, it was assumed that the strains along both in-plane components were equivalent ($\epsilon_x = \epsilon_y$). This assumption is, in some sense, an oversimplification. From a mechanical standpoint, the only points that satisfy this assumption are those which are situated on the middle edge z of the sample, and rigorously, ϵ_x is different from ϵ_y almost everywhere. On the other hand, ϵ_x is a result of an integrated measurement along the entire height of the sample. Thus, when measurements were performed along the z -axis, ϵ_x may be recognized as a representative value of the middle point of the transversal section and, hence, the hypothesis is applicable.

IV. FEM Analysis

A tridimensional thermal elastoplastic model was generated to study SiC-Mo joints. A preliminary analysis was performed considering both materials as ideally linear-elastic components. Subsequently, a model where only the ceramic was considered to be linear-elastic throughout the thermal loading was constructed. In this case, the metallic component was modeled considering an elastic-perfect-plastic behavior, the von Mises yield criterion, and the associative Prandtl-Reuss flow rule.

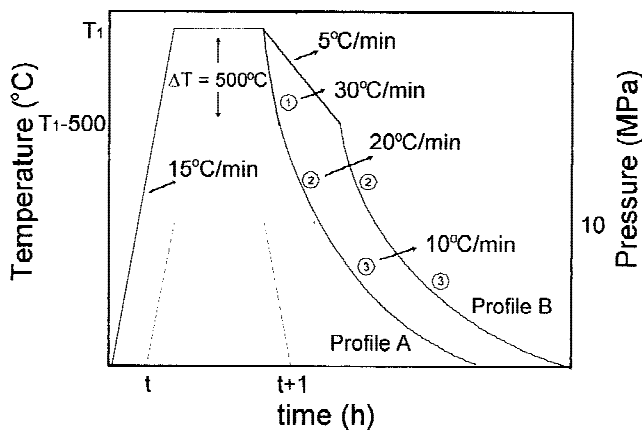


Fig. 1. Pressure and temperature profiles used to join SiC to molybdenum ($T_1 = 1200^\circ$ or 1400°C).

The software that was used (ANSYS 5.0, ANSYS, Houston, TX) allows this constitutive behavior to be modeled by using a kinematic hardening, as long as very low values of the tangent modulus (E_T) are used, such as in the present situation, i.e., $E_T/E = 0.05$.

Because of the large extension of the temperature range that has been considered (ambient to joining temperature), the dependence of the thermomechanical properties of the material on the temperature was considered (Fig. 2). Because the variation of the Poisson's ratio ν with the temperature is negligible for both SiC and molybdenum, they were considered to be constants.

The geometry of the modeled sample is schematically shown in Fig. 3. As a consequence of the symmetry of the sample, with respect to its geometry, mechanical properties, and loading, only one quadrant of the couple was modeled. A sequence of finite-element meshes was applied. Firstly, a uniform mesh composed of trilinear hexagonal elements was considered. Subsequently, to improve the accuracy of the analysis near the interface (region of stress concentration), a triquadratic mesh was considered, as shown in Fig. 3. The results reported herein were obtained using this mesh. Shear stresses also were obtained from the analysis but not included in the discussion, because the experimental counterpart was not available for comparison.

Sample cooling was assumed to occur free of any applied mechanical load. In addition, the temperature distribution inside the diffusion couple was assumed to be uniform, to avoid the need to solve a heat-transfer equation during the iterative process. This assumption is quite straightforward, because the cooling time in the furnace was sufficiently long, considering the thermal diffusivity of molybdenum ($4 \times 10^{-5} \text{ m}^2/\text{s}$) and the relatively small dimensions of the couple. To simplify the analysis, creep effects were not considered initially.

V. Results and Discussion

Initially, the distribution of residual stresses in SiC-Mo joints was studied via neutron diffraction along a line perpendicular to the SiC/molybdenum interfaces, as shown in Fig. 4(a). For the sample that was hot-pressed at 1200°C and cooled according to profile A, the maximum σ_x stress (330 MPa) was measured on the molybdenum side of the joint at a distance of 0.25 mm from the interface (Fig. 4(b)). On the SiC side, a corresponding value of -150 MPa was measured at an equivalent distance from the interface. SiC was in compression in the direction of σ_x , whereas molybdenum was in tension. Evidently, this occurrence was a result of the CTE mismatch between the materials. Molybdenum has a higher CTE than does SiC; therefore, it contracted more during cooling of the joint from the bonding temperature. However, its contraction was restrained by the bonding to the SiC, which resulted in compressive stresses on the ceramic side. Molybdenum reacted to that tendency, trying to extend the interface, thus resulting in a concentration of tensile stresses, especially near the interface with SiC. On both the ceramic and metal sides, the amplitude of σ_x decreased as the distance from the interface increased. On the SiC side, σ_x was almost zero at a distance of 1.5 mm, whereas on the molybdenum side, residual stresses were measured at an equivalent distance, as a result of the plastic deformation of the metal. In contrast, σ_z remained almost zero (within the margin of error) for most of the region that was analyzed, with an oscillating pattern that resulted in slight tension on the metal side and compression on the ceramic side. This behavior was confirmed via FEM analysis.

Increasing the joining temperature to 1400°C and using cooling profile A, the amplitude of σ_x adjacent to the interface increased to an average value of -550 MPa on the SiC side and 300 MPa on the molybdenum side (Fig. 5). Increasing the joining temperature from 1200°C to 1400°C increased the temperature variation to which the sample was exposed during cooling, which resulted in higher values of residual stresses, as

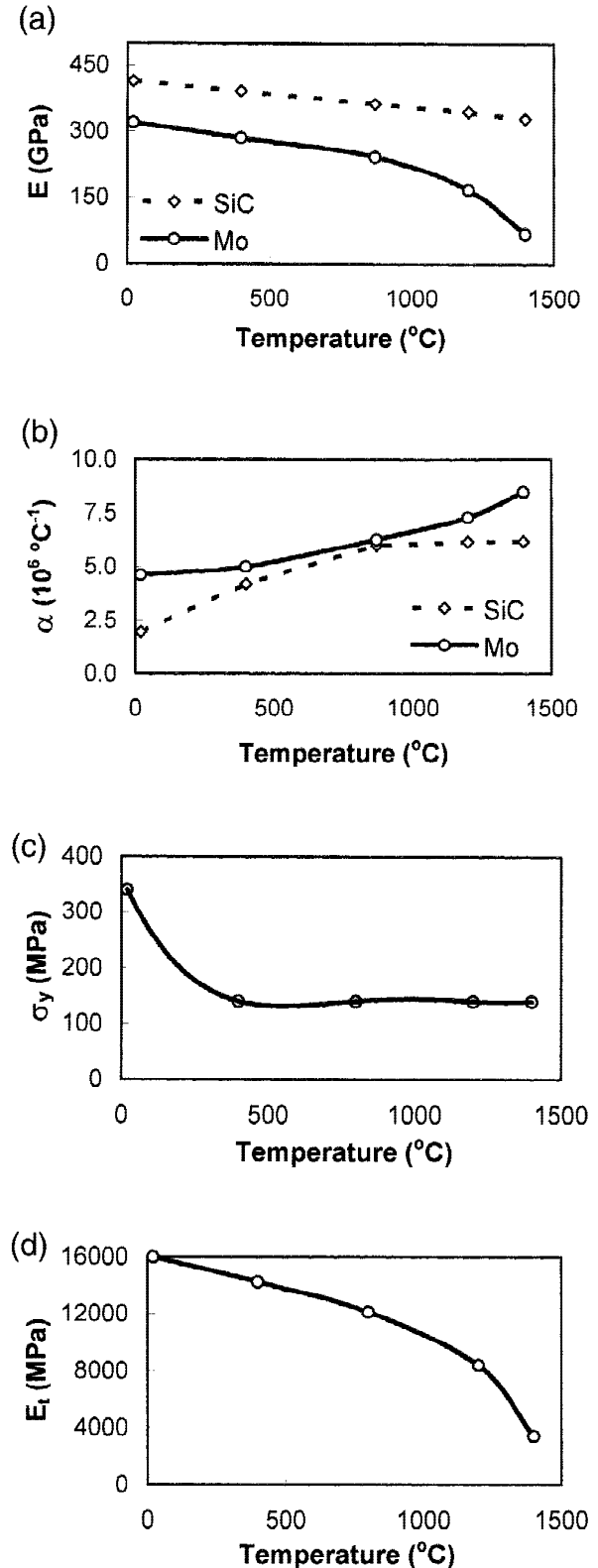


Fig. 2. Materials properties used to build the FEM model ((a) Young's modulus, (b) linear coefficient of thermal expansion, (c) yield strength of molybdenum, and (d) tangential modulus of molybdenum (from Refs. 12 and 13)).

a consequence of increased contraction. However, the stress distribution itself was similar to that obtained for the sample that was hot-pressed at 1200°C. A noticeable exception was the presence of high values of σ_z far from the interface. As the temperature increased, the compressive yield strength of molybdenum would decrease.¹³ However, because the mechanical

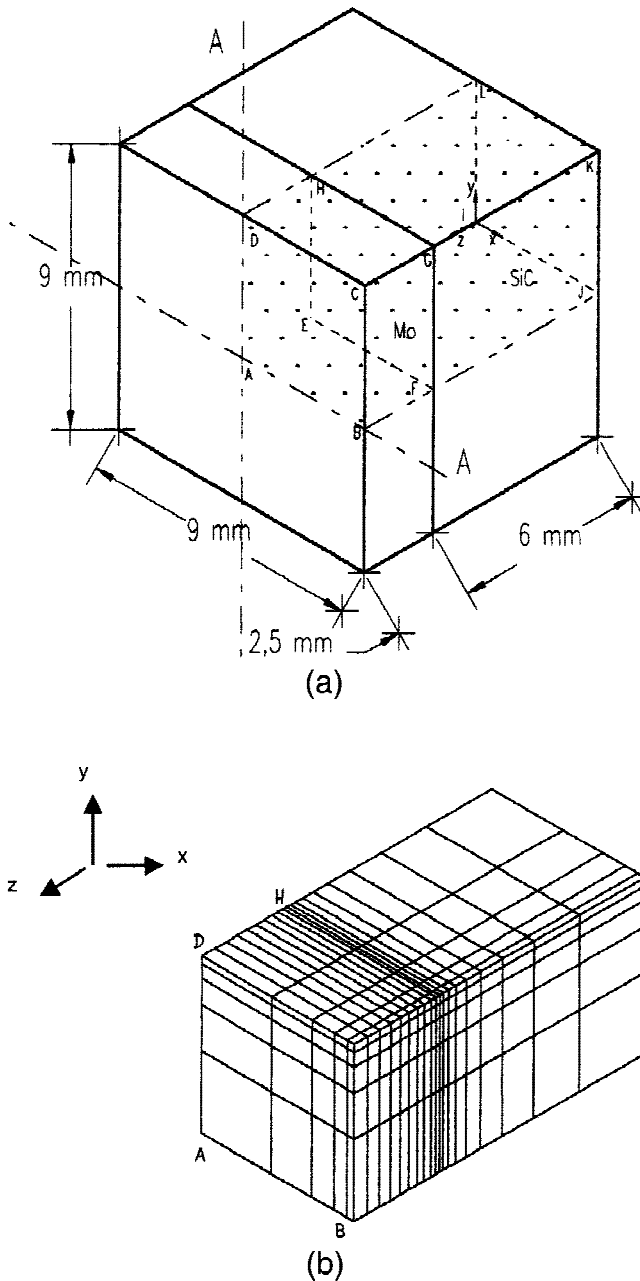


Fig. 3. Sample geometry modeled via FEM analysis.

pressure applied to the couple upon fabrication of the joint was set constant to 10 MPa, higher plastic deformation of the metal resulted at the higher joining temperature and, consequently, produced higher σ_z values.

The results that are depicted in Figs. 4 and 5 refer to samples that were furnace cooled from the joining temperature (cooling profile A). Figure 6 shows the stresses obtained from a sample that was hot-pressed at 1400°C and cooled according to profile B of Fig. 1. The stress distribution was similar to that represented in Fig. 5. However, the amplitude of compressive stresses on the SiC side of the joint adjacent to the interface, particularly for the σ_x component, was reduced significantly. Slow cooling (profile B) increased the time for which the sample was exposed to elevated temperatures. At high temperatures, atomic diffusion was sufficient to promote structural rearrangement of the materials and accommodating residual stresses through plastic deformation and creep. Therefore, controlled cooling should decrease the amplitude of σ_z in the SiC side, adjacent to the interface. Figure 5 provides clear evidence of this fact, because an average σ_x value of -550 MPa was

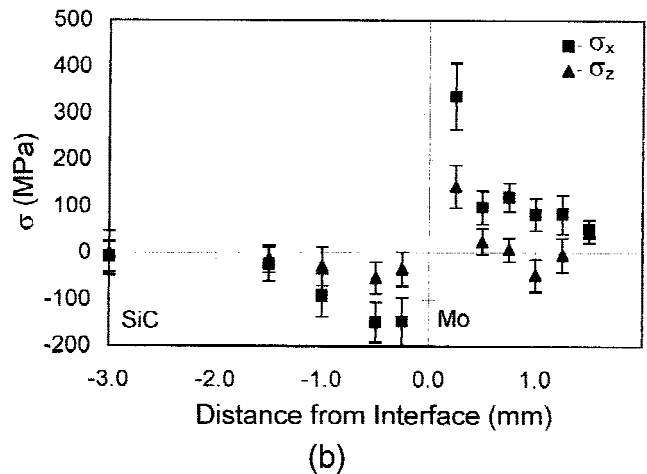
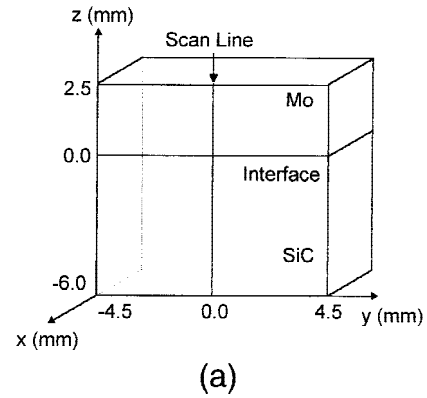


Fig. 4. (a) Position of scan line for neutron-diffraction analysis and (b) distribution of stresses across the SiC/molybdenum interface. Sample was hot-pressed at 1200°C and cooled according to profile A.

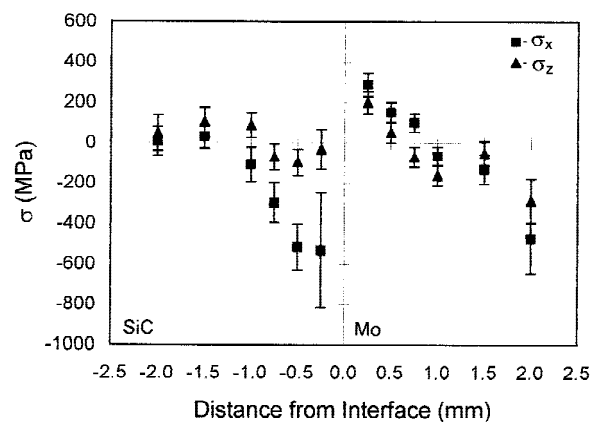


Fig. 5. Distribution of stresses across the SiC/molybdenum interface. Sample was hot-pressed at 1400°C and cooled according to profile A.

obtained under rapid cooling (profile A), whereas the amplitude of σ_x in the equivalent position in Fig. 6 (profile B) was almost zero, within the margin of error.

The distribution of residual stresses was then studied via FEM analysis. The calculation of stresses by using neutron-diffraction data and a mathematical approach involved different assumptions, which explained the major differences that were observed between the two set of results. To verify the assumptions that were made in the FEM analysis, an equivalent cylinder that had the same length and cross-sectional area as

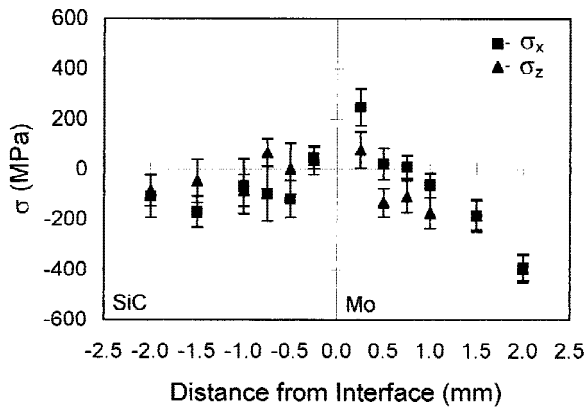


Fig. 6. Distribution of stresses across the SiC/molybdenum interface. Sample was hot-pressed at 1400°C and cooled according to profile B.

the original sample was modeled. Then, the problem was analyzed by using revolution symmetry and biquadratic finite elements. The results showed that the qualitative stress behavior was in good agreement with results published in the literature regarding the numerical analysis of a similar ceramic-metal system (Si₃N₄-SM50 steel).¹⁰ Then, the actual joint geometry was modeled. Several meshes were used in an attempt to reach a reasonable balance between accuracy and analysis cost. Although the calculated results always carry a dependence on the mesh that is used, this phenomenon becomes less significant as the mesh is optimized. In other words, the accuracy obtained herein is sufficiently adequate to conduct the intended comparison. Further refinements would increase the cost of the analysis without bringing any significant contribution to the study.

FEM analysis provides a complete map of all stress components (normal and shear) throughout the sample. Therefore, to perform a proper comparison with the values that are provided by the experimental technique, a convenient averaging of FEM values along the same pattern occupied by the neutron beam (the entire height of the sample along the *y*-axis) was performed.

Figure 7 shows a plot of the numerical results, along with the experimental values that were obtained via neutron diffraction for the sample that was joined at 1400°C. A reasonable agreement was observed between the experimental and calculated values for the σ_x component (Fig. 7(a)) on the SiC side of the sample. However, Fig. 7(b) reveals a clear difference between the values of σ_x and σ_y that were obtained from the FEM analysis on the molybdenum side, which contradicted the initial assumption that σ_x and σ_y were equal. Because the neutron-beam height covered all the sample height, the average result was assumed to represent the middle point of the cross section. Thus, each experimental stress value consisted of an average of the individual contributions of the elastic deformation components along the entire line corresponding to the sample height. In this case, by simple symmetry, ϵ_x and ϵ_y would be equivalent; thus, only one set of measurements was performed. Using the generalized Hooke's law, Eq. (3) and identical values of ϵ_x and ϵ_y yielded $\sigma_x = \sigma_y$. However, this assumption was an oversimplification, because the value of ϵ_x through the neutron beam is different from the average ϵ_y value. As was the case in Fig. 7(a), Fig. 7(c) shows a good agreement between the values of σ_z close to the interface only, on the SiC side of the sample. However, significant differences were observed on the molybdenum side, as well as on the SiC side far away from the interface. As noted earlier, the experimental stress values were computed by using average deformations and the generalized Hooke's law. In addition, another source of discrepancies for σ_z involves creep processes. The numerical model included the plastic behavior of the materials but excluded any consider-

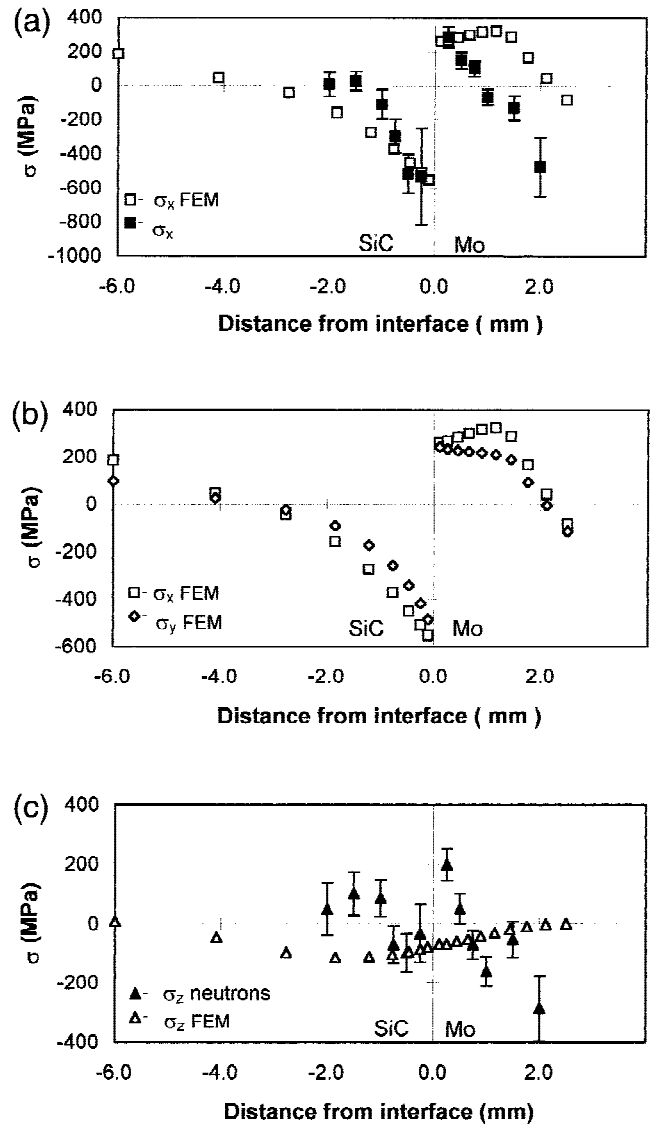


Fig. 7. (a) Neutron-diffraction and FEM results for σ_x , (b) FEM results for σ_x and σ_y , and (c) neutron-diffraction and FEM results for σ_z . The joining temperature was 1200°C.

ation of time-dependent processes; thus, creep of the molybdenum at high temperatures was not considered.

A brief calculation shows that any further improvement to the model should include creep effects. Estimation of the thermal, elastic, and plastic strain rate, respectively, yields

$$\alpha \left(\frac{dT}{dt} \right) \cong \frac{5.0 \times 10^{-6}}{K} \left(\frac{1400.0 \text{ K}}{3600 \text{ s}} \right) \cong 2 \times 10^{-6} \text{ s}^{-1} \quad (4)$$

$$\frac{1}{E} \left(\frac{d\sigma}{dt} \right) \cong \frac{300 \text{ MPa}}{3600 \text{ s}} \left(\frac{1}{325 \text{ GPa}} \right) \cong 2.6 \times 10^{-7} \text{ s}^{-1} \quad (5)$$

$$\frac{1}{E_T} \left(\frac{d\sigma}{dt} \right) \left(\frac{300 \text{ MPa}}{3600 \text{ s}} \right) \left(\frac{1}{16000 \text{ MPa}} \right) \cong 5.2 \times 10^{-6} \text{ s}^{-1} \quad (6)$$

On the other hand, considering a factor T/T_{melting} of 0.51–0.58 and a mean shear-stress value of ~150 MPa, the estimated value of the strain rate for molybdenum may be found within the range of 10^{-2} – 10^{-4} s⁻¹, which indicates that, for the temperature and load that are involved in the process, the viscous relief mechanism is much faster than the rate-independent plas-

ticity. The plastic deformation of molybdenum is characterized in the Appendix.

Considering the differences that have been encountered, a further refinement of the model including a viscoplastic approach would improve the confidence of the results and yield a better fit to the experimental data. Nevertheless, it was possible to evaluate the results and visualize the particular aspects and benefits of each approach, thus aiding in the interpretation of ceramic-metal stress analyses that are based on both experimental and FEM data.

VI. Conclusions

Thermomechanical residual stresses in SiC-Mo joints were studied via neutron diffraction and finite-element (FEM) analysis. Although differences were observed between the results generated by these methods, the comparison showed that the numerical and experimental techniques complemented each other in several aspects. As a result of diffusion bonding, high residual compressive stresses were observed on the SiC side of the joints. These stresses were counteracted by tensile stresses close to the interface on the molybdenum side. The distribution of stresses was affected by the cooling profile to which the diffusion couples were exposed. Slow cooling the samples during the first 500°C was an effective way to reduce the amplitude of the normal component of stress (σ_x), particularly within the SiC adjacent to the interface. For samples that were hot-pressed at 1400°C for 1 h, the σ_x value was reduced from -550 MPa to -50 MPa by controlling the cooling rate. The stress analysis via neutron diffraction considered that, as a consequence of the geometry of the sample, the normal and tangential components of strain (ϵ_x and ϵ_y , respectively) were equivalent. However, FEM analysis showed that this hypothesis was incorrect, and distinct values of σ_x and σ_y (σ_y is the tangential component of stress) were calculated. Finally, although the mathematical model considered the plastic deformation, it did not consider high-temperature creep. This omission resulted in significant differences between the calculated and experimental values that were obtained, especially on the molybdenum side of the joints.

APPENDIX

The plastic behavior of molybdenum was characterized using the associative bilinear kinematic hardening model that includes, as a particular case, the elastic-perfectly-plastic behavior. The yield surface used (F) is the von Mises criterion:

$$F(\sigma, \alpha) = \sigma_e - \sigma_y = \frac{3}{2}[(s - \alpha) \cdot (s - \alpha)]^{1/2} - \sigma_y = 0 \quad (\text{A-1a})$$

$$s = \sigma - \sigma_m \mathbf{I} \quad (\text{A-1b})$$

where σ_e is the von Mises equivalent stress and σ_y the unidimensional yield stress. The tensor α represents the center of the yield surface, s is the deviatoric stress tensor, $\sigma_m = \frac{1}{3} \text{tr}(\sigma)$ is the mean or hydrostatic stress, and \mathbf{I} is the identity matrix. The derivative of the yield surface gives

$$dF = \left(\frac{\partial F}{\partial \sigma} \right) d\sigma + \left(\frac{\partial F}{\partial \alpha} \right) d\alpha = 0 \quad (\text{A-2})$$

where

$$\sigma = D \epsilon^{\text{el}} \quad (\text{A-3})$$

$$d\epsilon^{\text{el}} = d\epsilon - d\epsilon^{\text{pl}} \quad (\text{A-4})$$

$$d\epsilon^{\text{pl}} = \lambda \frac{\partial F}{\partial \sigma} \quad (\text{A-5})$$

$$d\alpha = C d\epsilon = C d\epsilon^{\text{pl}} \quad (\text{A-6})$$

Here, D denotes the fourth-order elastic isotropic Hook tensor and ϵ^{el} and ϵ^{pl} are the elastic and plastic part of the infinitesimal strain ϵ , respectively. λ is the plastic multiplier, and C is a material constant that is dependent on the elastic modulus E and the tangent modulus E_T :

$$C = \frac{2}{3} \left(\frac{E E_T}{E - E_T} \right) \quad (\text{A-7})$$

In the particular case where $E_T = 0$, the classical ideal plastic model applies, i.e., $\alpha = 0$ and

$$F(\sigma, \alpha) = F(\sigma) = \frac{3}{2}[\sigma \cdot \sigma]^{1/2} - \sigma_y = 0 \quad (\text{A-8})$$

Acknowledgments: The authors would like to express the gratitude to all individuals involved in this study, particularly Prof. Paulo de Tarso R. Mendonça, Mr. André Klaubery, and Mr. Giovanni Dore for assisting in the development of the FEM model.

References

- K. Suganuma, "Reliability Factors in Ceramic/Metal Joining," *Mater. Res. Soc. Symp. Proc.*, **314**, 51-60 (1993).
- N. L. Loh and Y. L. Wu, "Diffusion Bonding of Ceramics to Metals," *Mater. Manuf. Processes*, **8** [2] 159-81 (1993).
- J. M. Howe, "Bonding, Structure, and Properties of Metal/Ceramic Interfaces," *Int. Mater. Rev.*, **38** [5] 257-71 (1993).
- A. E. Martinelli and R. A. L. Drew, "Microstructural Development during Diffusion Bonding of α -Silicon Carbide to Molybdenum," *Mater. Sci. Eng.*, **191A**, 239-47 (1995).
- W. J. Boettinger, J. H. Perepezka, and P. S. Frankwicz, "Application of Ternary Phase Diagrams to the Development of MoSi_2 -Based Materials," *Mater. Sci. Eng.*, **155A** [1-2] 33-44 (1992).
- F. J. J. Loo, F. M. Smet, G. D. Rieck, and G. Versoi, "Phase Relations and Diffusion Paths in the Mo-Si-C System at 1200°C," *High Temp.-High Pressures*, **14**, 25-31 (1982).
- A. Horiguchi, K. Suganuma, Y. Miyamoto, M. Shimada, and M. Koizumi, "Solid-State Interfacial Reaction in Molybdenum Carbide Systems at High Temperature-Pressure, and Its Application to Bonding Technique," *J. Soc. Mater. Sci. Jpn.*, **35** [388] 35-40 (1986).
- K. Kurokawa, "Interfacial Reactions of Metals and Alloys with Si-Based Ceramics," *Nippon Kinzoku Gakkai Kaihou*, **29** [11] 931-38 (1990).
- A. E. Martinelli, R. Berriche, and R. A. L. Drew, "Correlation between the Strength of SiC-Mo Diffusion Couples and the Mechanical Properties of the Interfacial Reaction Products," *J. Mater. Sci. Lett.*, **15** [4] 307-10 (1996).
- Y. C. Kim, T. Yamamoto, and T. H. North, "Generation and Reduction of Residual Stresses in Ceramic-Metal Joints," *Trans. JWRI*, **21** [2] 285-91 (1992).
- J. H. Root, J. D. Sullivan, and B. R. Marple, "Residual Stresses in Alumina-Mullite Composites," *J. Am. Ceram. Soc.*, **74** [3] 579-83 (1991).
- Engineered Materials Handbook, Vol. 4, *Ceramics and Glasses*. ASM International, Materials Park, OH, 1991.
- Metals Handbook*, Vol. 2, 9th Ed.; pp. 771-76. ASM International, Materials Park, OH, 1990. □